Advanced Physical Research
Vol.8, No.1, 2026, pp.140-151
https://doi.org/10.62476/apr.81140

CHARACTERIZATION STUDY OF GREEN SYNTHESIZED PMMA CNT Ag NANOCOMPOSITE STRUCTURAL OPTICAL ELECTRICAL AND THERMAL PERFORMANCE AS PROMISING OPTOELECTRONIC THIN FILMS

Sarah Imad Abdulraheem[1], **Hanaa Hussein Salman**[1], **Ishraq Abboodi Fadhil**[2], **Jamal Nasir Jabir**[1*], **Amjed Mirza Oda**[3]

[1]Department of Physics, College of Education, University of Al-Qadisiyah, Al-Qadisiyah, Iraq
[2]Department of Medical Physics, College of Science, University of Al-Qadisiyah, Al-Qadisiyah, Iraq
[5]Science Department, Basic Education College, University of Babylon, Babylon, Iraq

Abstract. The current study presents a green method for preparing polymethyl methacrylate/carbon nanotubes/silver nanoparticles (PMMA/CNT/AgNPs) nanocomposites through the use of eucalyptus leaf extracts as a biological reducing agent for Ag^{+} ions. Various amounts of AgNPs have been added to the PMMA/CNT nanocomposite to investigate its effects on structural, optical, and electrical properties. The process of fabrication consisted of dispersing multi-walled carbon nanotubes (MWCNTs) in acetone and mixing them with PMMA and AgNPs created in situ through a phytochemical reduction process. FTIR spectra showed the presence of functional groups in PMMA and evidence of interface reactions between CNTs and AgNPs. SEM images showed that AgNPs were mainly spherical and their dispersion depended on silver concentrations. UV-Vis spectra revealed the presence of localized Surface Plasmon Resonance peaks, resulting in enhanced absorption of visible light. Electrical characterization revealed enhanced DC as well as AC conductivity with the increase in AgNP concentration, due to the creation of conductive pathways. The present work emphasizes the combined use of the transparency offered by PMMA, the conductivity offered by CNTs, and the Ag plasmonic properties within a single nanocomposite material. The green synthesis method presented here provides a low-cost, scalable, and environmentally friendly alternative to the presently available chemical syntheses, making these nanocomposites attractive materials for the development of flexible electronics, optoelectronics, as well as low-frequency electromagnetic interference shielding.

Keywords: PMMA, CNT, AgNPs, Green Synthesis, Nanocomposites, Environmentally friendly.
Corresponding author: Jamal Nasir Jabir, Department of Physics, College of Education, University of Al-Qadisiyah, Al-Qadisiyah, Iraq, e-mail: *jamal.jabir@qu.edu.iq*
Received: 10 December 2025; Revised: 16 January 2026; Accepted: 21 January 2026; Published: 18 February 2026.

1 Introduction

Polymethyl methacrylate (PMMA) is a transparent thermoplastic polymer renowned for its optical clarity, environmental stability, and ease fabrication. With visible light transmittance reaching up to 99%, PMMA has found wide-ranging applications in optical and optoelectronic systems, including waveguides, optical switches, couplers, splitters, transceivers, hard contact lenses, luminous ceilings, and aerospace windows (Zidan & Abu-Elnader, 2005; Nassier & Shinen, 2022). Its low density, cost-effectiveness, and high volume productivity make it a strong

candidate for industrial-scale optical components. However, the intrinsic limitations of PMMA-including extremely low electrical conductivity, modest tensile strength, and limited visible light absorption - restrict its applicability in advanced electronic and photonic device (Goyal et al., 2017). To address these limitations, researchers have increasingly turned to polymer nanocomposites, in which conductive or optically active nanomaterials are embedded within the PMMA matrix to yield multifunctional performance (Petchthanasombat et al., 2012). Among various nanofillers, Ag-NPs have attracted significant attention due to their outstanding electrical conductivity, chemical stability, antibacterial activity, and strong LSPR in the visible spectrum. This plasmonic phenomenon enhances optical absorption and scattering, enabling applications in sensors, plasmonic devices, and EMI shielding (Duman et al., 2025; Butt et al., 2012; Loiseau et al., 2019). Separately, CNTs-both single-walled (SWCNTs) and MWCNTs—offer exceptional tensile strength, high thermal stability, and extraordinary electrical conductivity, which can be tailored via heteroatom doping (Stephan et al., 2000). When incorporate into PMMA, CNTs can form percolative conductive networks, significantly enhancing electrical transport while maintaining acceptable optical transparency (Alawi & Ali, 2023). Studies on PMMA/Ag nanocomposites (e.g., ref. (Goyal et al., 2017)) have shown notable improvements in optical absorption due to surface plasmon resonance (SPR) effects but only limited gains in conductivity, as metallic pathways remain discontinuous. Conversely, PMMA/CNT composites (e.g., ref. (Al-Osaimi et al., 2014)) demonstrate significant conductivity enhancements but lack plasmonic optical tuning. More recent research, including Hazim et al. (2021) and Alawi & Ali (2023), has investigated ternary PMMA/CNT/Ag systems, reporting synergistic improvements in both optical and electrical properties as well as EMI shielding capabilities. Nevertheless, most of these works rely on conventional chemical synthesis methods that employ hazardous reducing agents, are energy-intensive, and raise environmental and scalability concerns. Although the synergistic potential of combining Ag-NPs and CNTs in PMMA matrices is recognized, systematic studies using environmentally benign synthesis routes remain scarce. Green synthesis, employing plant-derived extracts as natural reducing agents, offers a sustainable alternative that minimizes toxic byproducts, reduces energy consumption, and enables scalable nanoparticle fabrication. Eucalyptus leaf extract, rich in polyphenolic compounds, has shown high efficiency in reducing Ag+ ions to stable metallic nanoparticles (Maji et al., 2017). However, there is limited literature addressing how green-synthesized Ag-NPs, in combination with CNTs, influencing the microstructure-property relationships in PMMA-based ternary nanocomposites. It should be emphasized that the novelty of the present work does not rely on the PMMA/CNT/Ag system itself, which has been previously reported, but rather on the environmentally begin synthesis route herein. The use of eucalyptus leaf extract as a natural reducing and stabilizing agent enables in-situ formation of Ag NPs without toxic chemicals, offering improved sustainability, lower environmental impact, and potential advantages in dispersion and interfacial compatibility. To the best of the author's knowledge, systematic investigations correlating green-synthesized Ag NPs with the optical, electrical and thermal performance of PMMA/CNT-based ternary nanocomposites remain limited. The present study aims to bridge this gap by developing PMMA/CNT/Ag nanocomposites through a green synthesis route using eucalyptus leaf extract as the reducing agent for Ag-NPs. By systematically varying silver content and employing comprehensive characterization techniques-Fourier-transform infrared spectroscopy (FTIR), scanning electron microscopy (SEM), UV-Vis spectroscopy, differential scanning calorimetry (DSC), and DC/AC electrical measurements-this work elucidates the correlation between nanoscale structural features, plasmonic optical behavior, and electrical transport mechanisms. The findings will contribute to the achievement of multifunctional, eco-friendly nanocomposites for flexible electronics, optoelectronic devices, and EMI shielding applications.

2 Materials and Methods

2.1 Materials

Analytical-grade PMMA was procured from Merck (Germany), serving as the polymer matrix. MWCNTs were supplied by Cheap Tubes Inc. (USA) and utilized as the primary conductive nanofiller. Silver nitrate (AgNO3, $\geq$ 99% purity) was obtained from Sigma-Aldrich (USA) as the silver precursor. Dried Eucalyptus leaves, sourced from local markets, were employed as a phytochemical reducing and stabilizing agents in the green synthesis of Ag-NPs. Acetone (Merck, analytical grade) was used as the organic solvent, and double-distilled water (DDI) was used in all aqueous preparations.

2.2 Preparation of Eucalyptus Leaf Extract

The green reducing agents was prepared by finely grinding 1 g of dried Eucalyptus leaves and dispersing them in 25 mL of acetone. The mixture was agitated thoroughly until a dark brown coloration indicated the release of phytoconstituents rich in polyphenolic compounds. The suspension was then filtered to remove planet residues, yielding a clear extract, subsequently stored under refrigeration prior to use.

2.3 Synthesis of PMMA/CNT/Ag Nanocomposites

Three formulations of PMMA/CNT/Ag nanocomposites were prepared following a green synthesis approach. Initially, three PMMA solutions were prepared by dissolving 1.0 g of standard PMMA in 20 mL of acetone each, followed by continuous magnetic stirring for 1 h to obtain homogenous solutions. Separately, 0.02 g of CNT powder was dispersed in 50 mL of acetone using an ultrasonic probe for 10 min to ensure proper de-agglomeration. A portion of 10 mL from the CNT dispersion was then added to each PMMA solution and manually shaken to achieve uniform blending. Silver precursor solutions were prepared by dissolving 0.2 g of AgNO3 in 20 mL of acetone to obtain a 1mM stock solutions, stirred mechanically for 30 min. Different volumes (1, 3, and 6 mL) of this AgNO3 solutions were added separately to the three PMMA/CNT mixtures, producing formulations with varied Ag content. For the green synthesis of Ag-NPs, Eucalyptus leaf extract was used as a reducing agent. The extract was prepared by mixing 1 g of ground leaves with 25 mL of acetone until a dark brown coloration appeared; the mixture was then filtered to obtain a clear extract. Subsequently, 4 mL of the extract was added to each PMMA/CNT/AgNO3 mixture. The resulting blends were heated at 60 oC under continuous stirring, where the visible color change from grey to dark brown confirmed the in-situ reduction of Ag+ ions to metallic Ag-NPs. Finally, 5 mL of each viscous mixture was cast into separate Petri dishes and dried under ambient conditions to obtain thin films of PMMA/CNT/Ag nanocomposites. These films were characterized using SEM for surface morphology, FTIR for chemical interactions, DSC for thermal stability, UV-Vis spectroscopy for optical properties, and DC/AC conductivity measurements for electrical behavior. Figure 1 illustrates the visual appearance of the final films, showing a clean transition in color from grey (Ag1) to dark brown (Ag6) as the Ag-NPs concentration increases, thereby providing preliminary evidence of NP formation within the polymer matrix.

Fig.1: Digital photographic of the synthesized PMMA/CNT/Ag nanocomposites thin films, showing gradual color variation from gray to dark brown with increasing AgNPs concentration.

2.4 Characterization Techniques

The PMMA/CNT/Ag nanocomposite films underwent comprehensive characterization to establish the relationship between their structure and functional properties. Fourier transform infrared spectroscopy (FTIR) was used to identify the characteristic absorption bands of PMMA and to detect spectral variations associated with interactions between the polymer matrix, CNTs, and Ag-NPs. Scanning electron microscopy (SEM) provided detailed insights into surface morphology, NP distribution, and agglomeration patterns. Optical measurements using UV-Visible spectroscopy in the 200-800 nm range enabled the assessment of transmittance, absorption behavior, and LSPR features attributed to Ag-NPs. Thermal behavior was evaluated through differential scanning calorimetry (DSC) to determine phase transitions and thermal stability. Electrical performance was examined via DC conductivity tests and AC impedance spectroscopy over a frequency range of 100 Hz to 5 MHz, with precise film thickness measurements obtained using a digital micrometer to ensure accuracy in conductivity calculations.

3 Results and Discussion

3.1 Optical Properties of PMMA/ CNT/ Ag Nanocomposite

A. Surface Morphology (SEM Analysis)

SEM investigations provided clear insights into the effect of Ag-NP loading on the surface morphology of PMMA/CNT/Ag nanocomposites. At low Ag concentration (Ag1), Ag-NPs were uniformly distributed within the polymer matrix and along CNT surfaces, with minimal evidence of clustering, as shown in Figures 2(a, b, and c). This homogeneous dispersion indicates efficient reduction and stabilization by the Eucalyptus extract, ensuring strong interfacial interactions. At intermediate loading (Ag3), the morphology evolved into a partially agglomerated subsurface structure, where Ag-NPs tended to cluster while remaining embedded in the polymer. Distinct separations between the polymer, CNTs and Ag domains were evident, reflecting reduced compatibility at higher filler content. Although such agglomeration compromises uniformity, it contributes to the formation of conductive islands that enhance charge transport (Fenta & Mebratie, 2024). At higher Ag content (Ag6), pronounced agglomeration became dominant, with larger particulate domains observed on the polymer surface. These clusters disrupt film homogeneity and decrease transparency but create continuous conductive networks that significantly improve electrical conductivity. Collectively, the SEM analysis confirms a clear morphological from uniform dispersion (Ag1), partial subsurface clustering (Ag3), and large scale agglomeration (Ag6). This progressive change illustrates the critical role of Ag loading in dictating the balance between structural uniformity, optical clarity, and electrical performance of the nanocomposites.

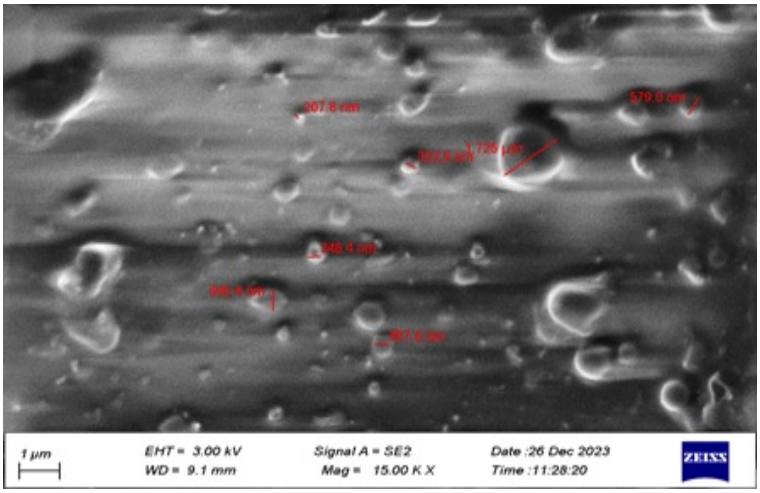

Fig.2(a): SEM micrograph of PMMA/CNT/Ag1 nanocomposite showing uniform distribution of AgNPs within the polymer matrix.

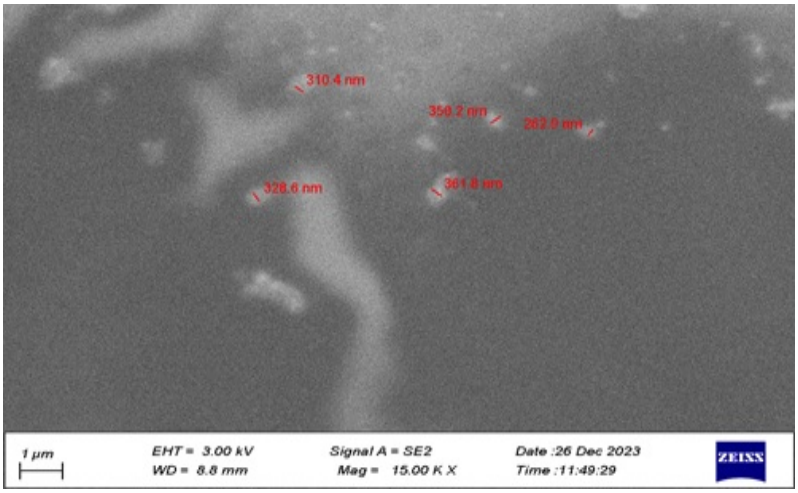

Fig.2(b): SEM micrograph of PMMA/CNT/Ag3 nanocomposite indicating agglomerated subsurface particulate structures and separation between polymer, CNTs, and AgNPs.

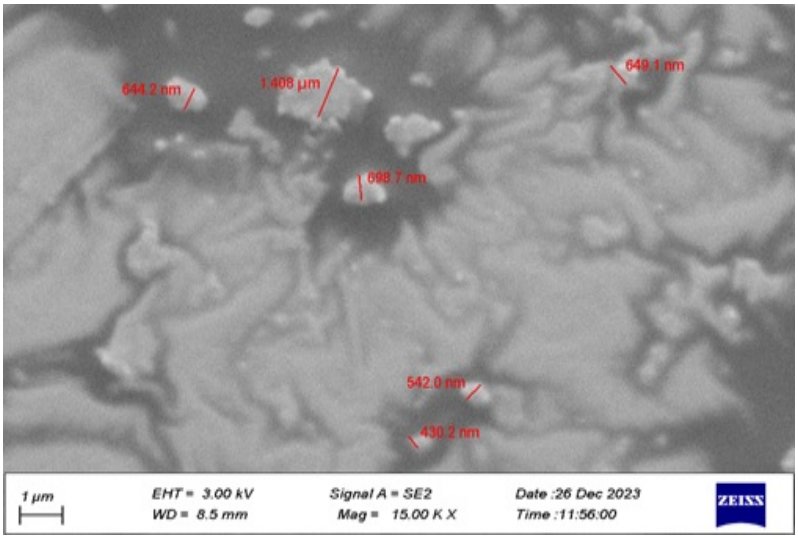

Fig.2(c): SEM micrograph of PMMA/CNT/Ag6 nanocomposite displaying partial nanoparticle aggregation at higher Ag concentration, affecting homogeneity.

B. Fourier-transform infrared Analysis (FTIR)

The FTIR spectra of PMMA/CNT/Ag nanocomposites provided strong evidence of molecular interactions between the polymeric matrix, CNTs, and AgNPs, as verified in figure 3. The main chemical structure of PMMA contains prominent C-O and C=O (carbonyl) groups. CNT are composed of non-polar C-C bonds and typically do not produce obvious characteristic peaks in FTIR pattern. Nevertheless, the essential role of embedding CNT into composites is primarily to enhance their mechanical or electrical properties. Likewise, the incorporated AgNPs do not contribute by evident chemical bonds within the FTIR spectrum. However, involving Ag as fillers indirectly affect the functional groups peaks of PMMA via physically interacting across the polymer's bonds. The major peaks in FTIR spectrum in the three samples are most likely from PMMA backbone chains. The strong, sharp absorbance peaks around 1745 cm^{-1} are characteristic of the stretching vibration of C=O (carbonyl) group in PMMA. The slight peak shifts obviously appeared in the three curves may suggest inconsiderable interactions between the local chemical bonds of PMMA and AgNPs were occurred. Additionally, the peak at ∼1637cm^{-1} was assigned to C=O stretching and overlapped with the O-H bending vibrations, further confirming chemical interactions within the composite. The weak absorption peak at 1539 cm-1, attributed to the C-C stretching mode of CNTs, diminished progressively with increasing Ag content, implying, that AgNPs were effectively deposited on CNT surfaces and partially masked their vibrational signatures. The sharp characteristic band at ∼1240 cm-1 is typically associated with the stretching vibration of the ester group C-O in PMMA structure. A distinct band at 2924 cm-1 was assigned to asymmetric C-H stretching vibrations of methyl groups. In the sample Ag6, additional C-O stretching was detected at 3415 cm-1, possibly reflecting enhanced hydrogen bonding interactions at higher Ag content. The detected changes in the intensity and shifting of the key peaks, especially the conspicuous C=O peak, confirm that the AgNPs have effectively integrated with the polar functional groups of PMMA and CNT. Significantly, such interactions motivate stabilization of nanoparticles within the composite and play a crucial role in tailoring the optical and electrical properties of the nanocomposites.

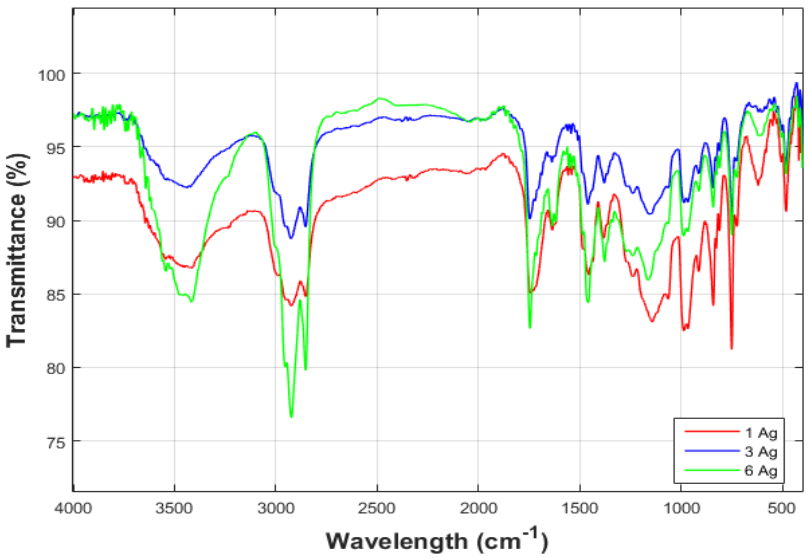

Fig.3: FTIR spectra of PMMA/CNT/Ag nanocomposites at different Ag loading (Ag1, Ag3, Ag6), indicating characteristic peaks of C=O, O-H, and C-C groups, confirming interfacial interactions.

C. Ultraviolet-Visible Analysis

UV-Visible spectroscopy was employed to investigated the optical behavior of the optical behavior of the synthesized PMMA/CNT/Ag nanocomposites in the wavelength range of 200-800 nm. Pure PMMA films exhibited high transmittance across the visible spectrum, reflecting their inherent optical transparency (Fadhil et al., 2025). The incorporation of CNTs introduced

additional absorption features in the near-UV region, which can be attributed to π- π^* electronic transitions within the conjugated carbon framework of the nanotubes (Al-Osaimi et al., 2014). A distinct surface plasmon resonance (SPR) peak characteristic of Ag-NPs emerged at approximately 420 nm in all Ag-containing samples. The intensity of this SPR band increased progressively with Ag-content (Ag1<Ag3<Ag6), confirming the in-situ reduction of Ag+ to metallic Ag-NPs and their successful integration into the polymer matrix. The sharpness of the SPR feature further indicates good NP dispersion, particularly at lower concentrations. Notably, the absorption edge of the composites showed a slight redshift as the Ag loading increased, suggesting a narrowing of the optical bandgap. This phenomenon is typically associated with enhanced electronic interactions and the introduction of localized states in the band structure due to NP incorporation (Hazim et al., 2021). Such bandgap tailoring is of great significance for optoelectronic applications, as it facilitates improved charge transfer and light-matter interactions. Although the film became progressively darker with increasing Ag content, as visually evident in figure 4, sufficient transmittance was retained in the visible region, making them suitable for optical and photonic applications. These findings demonstrate a synergistic enhancement of optical properties through the combined effect of CNTs (broadband absorption) and AgNPs (plasmonic resonance). The appearance of the SPR based around 420 nm is consistent with the formation of spherical AgNPs with an expected size range of approximately 20-40nm, as reported in green-synthesized AgNPs systems. Although direct particle size measurements such as TEM or XRD were not available in this study, the SPR position, intensity evolution, and SEM observation collectively confirm the successful reduction of Ag+ ions and effective incorporation of AgNPs within the polymer matrix.

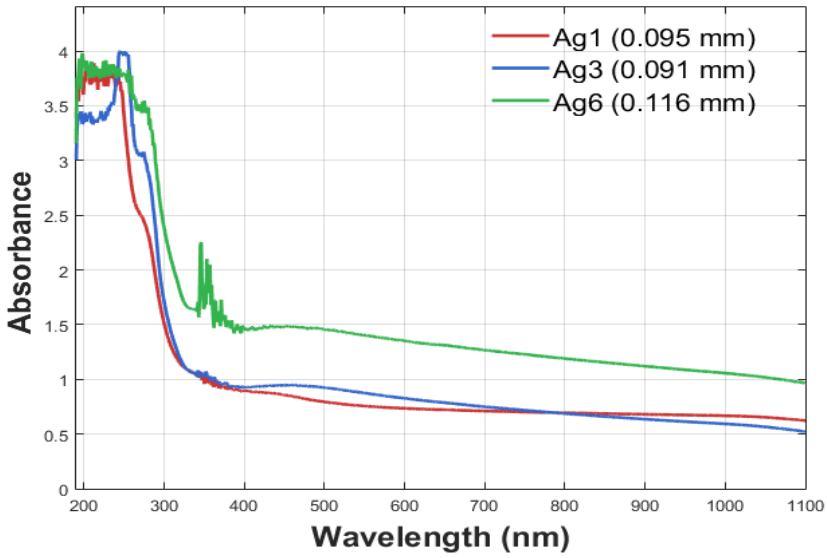

Fig.4: UV-Vis absorption spectra of PMMA/CNT/Ag showing a distinct surface plasmon resonance peak around 420 nm and bandgap narrowing with higher Ag content.

3.2 Electrical Properties of PMMA/ CNT/ Ag Nanocomposite

The electrical characteristics of the PMMA/CNT/Ag nanocomposite film were evaluated through resistivity and conductivity measurements. The resistivity (ρ) was calculated using the relation: ρ=$R.A/L$, where R is the measured electrical resistance of the sample, A is the cross-sectional area of the film, and L is the film thickness. The corresponding DC conductivity (σ_{DC}) was obtained as: σ_{DC}=$1/\rho$=$L/R.\ A$. The temperature dependence of conductivity was analyzed using the Arrhenius equation: $\sigma_{DC}(T)$ =σ_0 exp(E_a/K_BT), where σ_0 is the pre-exponential factor, E_a is the activation energy, K_B is the Boltzmann's constant, and T is the absolute temperature. By plotting ln(σ_{DC}) against ($1/T$), the activation energy was determined from the slope. The total

conductivity as a function of frequency was calculated from: $\sigma_t(\omega) = L/R.\ A$. The AC conductivity ($\sigma_{AC}$) was separated from the total conductivity according to: $\sigma_{AC}(\omega) = \sigma_t(\omega) - \sigma_{DC} = A\omega^s$, where $\omega = 2\pi f$ is the angular frequency, A is a temperature-independent constant, and $s(0<s<1)$ is the frequency exponent (Alawi & Ali, 2023; Al-Lamy et al., 2020). Figure 5 illustrates the variation of DC conductivity with temperature for PMMA/CNT/Ag nanocomposites. A clear increase in conductivity with rising temperature is observed across all samples, confirming a semiconductor behavior governed by thermally activated charge transport. At 20 °C, conductivity values are relatively low (∼1.3-1.6 ×10-5 S/cm), but they increase steadily, reaching ∼2.2×10-5 S/cm (Ag1), 2.8×10-5 S/cm (Ag3), and 3.9×10-5 S/cm (Ag6) at 60 °C. The enhancement is most pronounced for the Ag6 sample, indicating that higher Ag content promotes the formation of conductive pathways within the PMMA matrix. This trend is consistent with the percolation model, where increasing filler content enhances electron hopping between localized states along the CNT-Ag network. Figure 6 show the AC conductivity response as a function of frequency (100 Hz – 10 MHz). All samples exhibit the typical Jonscher's power –law behavior, where σ_{ac} increases gradually at low-to-mid frequencies and sharply beyond ∼104 Hz. This behavior is attributed to hopping and tunneling conduction of charge carriers facilitates by alternating electric field. Interestingly, at higher (>106 Hz), the Ag1 and Ag3 samples exhibit higher conductivity (approaching 1 S/cm) compared to Ag6, which shows lower σ_{ac} (∼10-3 - 10-2 S/cm). This anomaly can be linked to the agglomeration of Ag-NPs in the Ag6 sample, as revealed by SEM analysis, which reduces the effective number of conductive channels despite the higher filler loading. At high frequencies, excessive AgNPs agglomeration in the Ag6 sample reduces the effective number of hopping sites and interfacial polarization regions, leading to suppressed AC conductivity despite higher metallic content. In contrast, Ag1 and Ag3 demonstrate more uniform NP dispersion, leading to improved high-frequency conductivity.

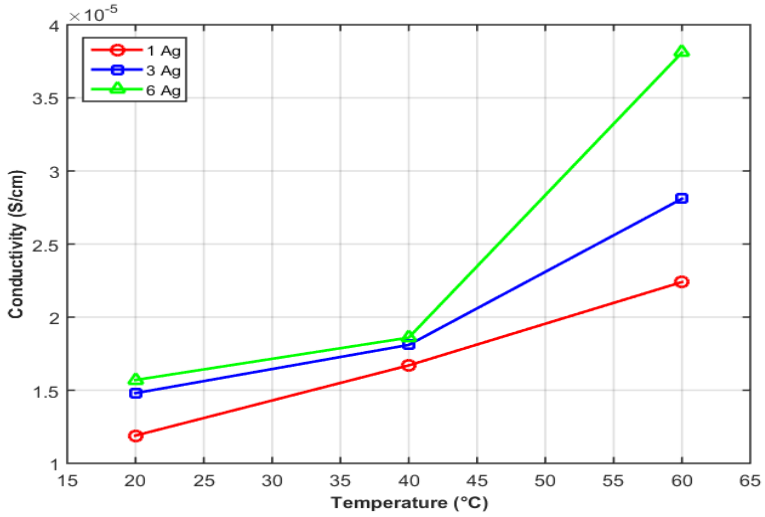

Fig.5: Temperature dependence of DC conductivity for PMMA/CNT/Ag nanocomposites, showing thermally activated conduction consistent with the Arrhenius model.

The combined DC and AC measurements confirm that conductivity in PMMA/CNT/Ag nanocomposites is strongly dependent on Ag loading and dispersion state. While higher Ag content enhances DC conductivity due to increased percolation pathways, excessive loading (Ag6) induces particle agglomeration that reduces AC conductivity at high frequencies. Thus, optimal dispersion at intermediate Ag loading (Ag3) offers a balance between conductivity and structural homogeneity. These finding align with reported trends in polymer nanocomposites, where the synergy between CNTs and Ag-NPs enhances both temperature-activated conduction and frequency-dependent hopping transport, making these systems promising candidates for flexible electronic devices and low-frequency EMI attenuation applications (Alawi & Ali, 2023;

Yakuphanoglu et al., 2010; Kazemian Abyaneh et al., 2011).

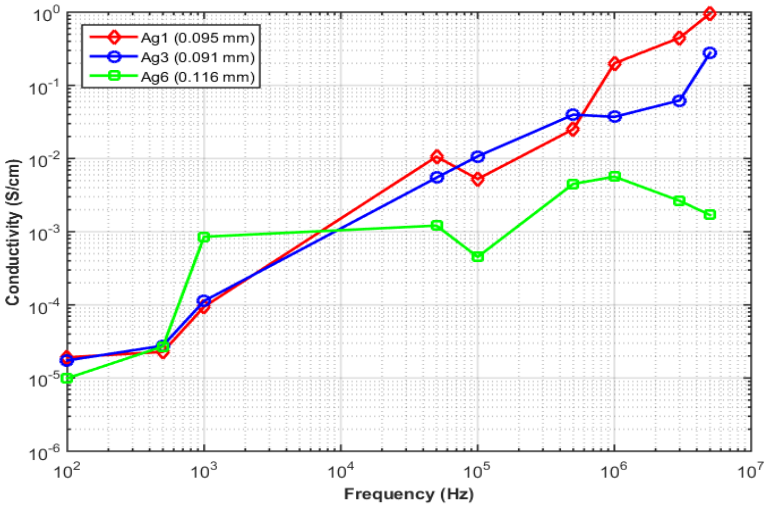

Fig.6: AC conductivity spectra of PMMA/CNT/Ag nanocomposites fitted with Jonscher's power law, highlighting frequency-dependent hopping transport.

3.3 Thermal Properties of PMMA/CNT/Ag Nanocomposites

The thermogravimetric analysis (TGA), Fig. 7(a) show the thermal decomposition behavior of the nanocomposites with varying Ag content. All samples display a two-step weight loss; first stage (∼100-200 °C), attributed to moisture removal and the volatilization of residual solvents or low-molecular weight fractions. Second stage (∼350-450) °C, corresponds to the main chain scission of PMMA and degradation of organic functional groups. The onset decomposition temperature (Tonset) increased slightly with higher Ag loading. For instance, Ag1 degraded around ∼365 °C, while Ag6 shifted closer to ∼380 °C, indicating that Ag NPs act as a thermal stabilizer by restricting chain mobility and providing heat dissipation sites. Similar stabilization effects of Ag in PMMA have been reported by (Cao et al., 2025). The differential scanning calorimetry (DSC), as in Fig.7(b), revealed clear differences in the glass transitions temperature (Tg) with increasing Ag loading. Pure PMMA typically shows Tg around 105 °C, but in the composites, Tg values exhibited a slight upward shift (e.g., Ag1≈110 °C, Ag6≈113 °C). This increased suggests stronger interfacial interactions PMMA chains, CNTs, and Ag NPs, which hinder the mobility of polymer segments. Furthermore, the DSC curves displayed endothermic peaks related to polymer relaxation and possible nanoparticle-matrix interactions. The enhanced Tg with increasing Ag content corroborates FTIR findings, where chemical bonding (C=O, O=H) indicating improved polymer-filler adhesion.

The derivative thermogravimetry (DTG), curves in Fig.7(c), provided insight into the rate of decomposition. The maximum decomposition rate temperature (Tmax) also shifted toward higher values with increasing Ag content. For example, Ag1 exhibited Tmax∼375°C, whereas Ag6 shifted above 390 °C. This confirms that the incorporation of Ag-NPs delays the degradation process, further supporting their role as thermal stabilizers. Additionally, the DTG peak intensities decreased with higher Ag loading, implying a slower degradation rate. This can be explained by the barrier effect of CNTs combined with the heat absorption capacity of Ag-NPs, which together suppress thermal decomposition. The TGA, DSC, and DTG results collectively demonstrate that incorporating CNTs and Ag-NPs into PMMA significantly enhances thermal stability. The improvements can be attributed to; (1) NP barrier effects that hinder the diffusion of volatile decomposition products. (2) strong interfacial bonding (as confirmed by FTIR) that restricts polymer chain mobility. Heat dissipation by metallic Ag-NPs, which delays the onset of degradation. These finding are in strong agreement with previous studies on polymer/metal

nanocomposites (Goyal et al., 2017; Cao et al., 2025). Overall, the incorporation of CNTs and Ag not only improves the optical and electrical properties but also provides a substantial enhancement in thermal stability, making these nanocomposites attractive for high-performance applications in electronics, coatings, and thermal management systems. These thermal analysis results (TGA, DSC, and DTG) are summarized in Table 1.

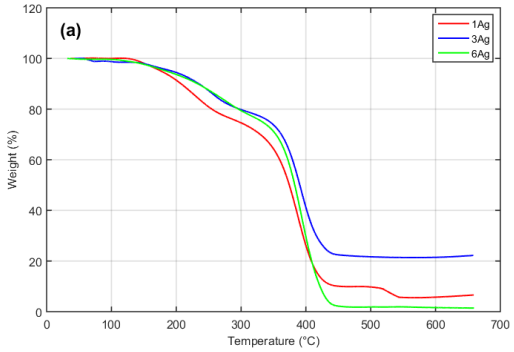

Fig.7(a): TGA thermogram of PMMA/CNT/Ag nanocomposites, illustrating improved thermal stability and delayed decomposition with increasing Ag loading.

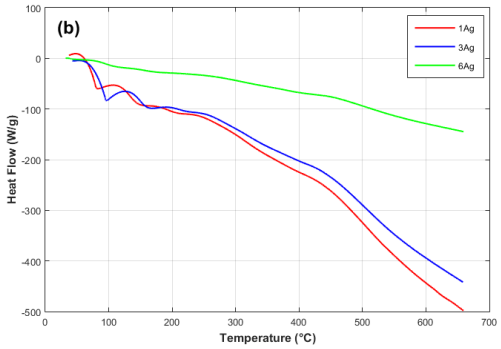

Fig.7(b): DSC thermograms of PMMA/CNT/Ag nanocomposites showing a gradual increase in glass transition temperature (Tg) with higher Ag concentration, indicating restricted polymer chain mobility.

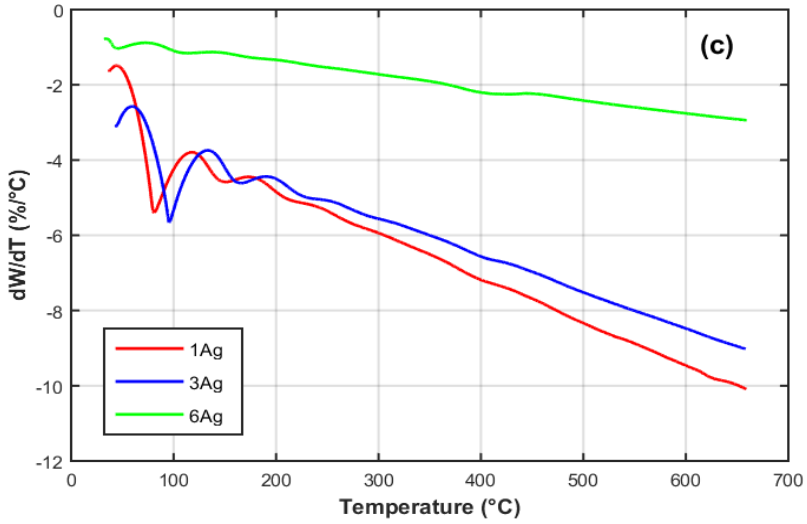

Fig.7(c): DTG curves of PMMA/CNT/Ag nanocomposites demonstrating a shift of maximum decomposition rate temperature (Tmax) toward higher values with Ag loading, confirming enhanced thermal resistance.

Table 1: Thermal parameters of PMMA/CNT/Ag nanocomposites.

Sample	**Tonset (°C)**	**Tmax (°C)**	**Tg (°C)**
Ag1	**∼365**	**∼375**	**∼110**
Ag3	**∼372**	**∼382**	**∼112**
Ag6	**∼380**	**∼390**	**∼113**

4 Conclusion

The PMMA/CNT/Ag nanocomposites have been successfully developed through the application of green chemistry techniques, making use of the natural reducing agent, eucalyptus extract. Structural analysis by FTIR and SEM has provided evidence for strong interfacial interactions and the shift from well-dispersed AgNPs to aggregated particles as the Ag content is increased. UV-Vis analysis has provided evidence for the development of SPR and the reduction in the band gap, reflecting increased optical activities. Conductivity analysis has provided evidence for activated DC and frequency-dependent AC behaviors that follow the conducting hopping process, and the highest performances have been achieved at intermediate Ag concentrations. Finally, the analysis by TGA, DSC, and DTG has provided evidence for enhanced thermal stability, as evidenced by the delay in degradation and the increase in the values of Tg and Tmax. These findings collectively point to the potential use of PMMA/CNT/Ag nanocomposites developed by applying environmentally friendly techniques as versatile materials for flexible optoelectronics and promising EMI shielding applications at low frequencies. Although direct measurements for AgNPs size have been avoided, evidence for successful AgNPs synthesis and integration into the polymer matrix has been provided by SEM and optical analysis.

References

Alawi, B.I., Ali, N.A. (2023). Improvement of the shielding effectiveness of PMMA/MWCNTs/Ag hybrid composite for X-band application. *East European Journal of Physics*, 2, 206-214.

Al-Osaimi, J., Al-Hosiny, N., Abdallah, S., & Badawi, A. (2014). Characterization of optical, thermal and electrical properties of SWCNTs/PMMA nanocomposite films. *Iranian Polymer Journal, 23*(6), 437-443.

Al-Lamy, H.K., Nasir, E.M., & Abdul-Ameer, H.J. (2020). Electrical properties of Cdxse1-x films at different thickness and annealing temperatures. *Digest Journal of Nanomaterials and Biostructures, 15*(1), 143-156.

Butt, F.K., Cao, C., Khan, W.S., Ali, Z., Mahmood, T., Ahmed, R., ... & Nabi, G. (2012). Fabrication of novel SnO2 nanofibers bundle and their optical properties. *Materials Chemistry and Physics, 136*(1), 10-14.

Duman, H., Eker, F., Akdaşçi, E., Witkowska, A.M., Bechelany, M., & Karav, S. (2024). Silver nanoparticles: A comprehensive review of synthesis methods and chemical and physical properties. *Nanomaterials, 14*(18), 1527.

Fadhil, I.A., Abdulraheem, S.I., Mohammed, I.H., & Oda, A.M. (2025). Influence of Adding Silver Nanoparticles on Structural and Optical Characteristics of PMMA Nanopowders for Antibacterial Applications. *Iraqi Journal of Applied Physics, 21*(2), 286-290.

Fenta, E.W., Mebratie, B.A. (2024). Advancements in carbon nanotube-polymer composites: Enhancing properties and applications through advanced manufacturing techniques. *Heliyon, 10*(16).

Goyal, A., Sharma, A., Saini, I., Chandak, N., & Sharma, P. (2017). Tailoring of optical and electrical properties of PMMA by incorporation of Ag nanoparticles. *Bulletin of Materials Science, 40*(4), 615-621.

Hazim, A., Hashim, A., & Abduljalil, H. (2021). Fabrication of novel (PMMA-Al2O3/Ag) nanocomposites and its structural and optical properties for lightweight and low cost electronics applications. *Egyptian Journal of Chemistry, 64*(1), 359-374.

Kazemian Abyaneh, M., Jafarkhani, S., & Kulkarni, S.K. (2011). Electrical transport behaviour of silver–PMMA nanocomposite films at low temperature. *Journal of Experimental Nanoscience, 6*(2), 159-173.

Loiseau, A., Asila, V., Boitel-Aullen, G., Lam, M., Salmain, M., & Boujday, S. (2019). Silver-based plasmonic nanoparticles for and their use in biosensing. *Biosensors, 9*(2), 78.

Maji, P., Choudhary, R. B., & Majhi, M. (2017). Structural, electrical and optical properties of silane-modified ZnO reinforced PMMA matrix and its catalytic activities. *Journal of Non-Crystalline Solids,* 456, 40-48.

Morsi, M.A., Pashameah, R.A., Sharma, K., Alzahrani, E., Farea, M.O., & Al-Muntaser, A.A. (2023). Hybrid MWCNTs/Ag nanofiller reinforced PVP/CMC blend-based polymer nanocomposites for multifunctional optoelectronic and nanodielectric applications. *Journal of Polymers and the Environment, 31*(2), 664-676.

Nassier, L.F., Shinen, M.H. (2022). Study of the optical properties of poly (methyl methacrylate)(PMMA) by using spin coating method. *Materials Today: Proceedings*, 60, 1660-1664.

Petchthanasombat, C., Tiensing, T., & Sunintaboon, P. (2012). Synthesis of zinc oxide-encapsulated poly (methyl methacrylate)–chitosan core–shell hybrid particles and their electrochemical property. *Journal of Colloid and Interface Science, 369*(1), 52-57.

Stephan, C., Nguyen, T.P., De La Chapelle, M.L., Lefrant, S., Journet, C., & Bernier, P. (2000). Characterization of singlewalled carbon nanotubes-PMMA composites. *Synthetic Metals, 108*(2), 139-149.

Yakuphanoglu, F., Yahia, I.S., Barim, G., & Senkal, B.F. (2010). Double-walled carbon nanotube/polymer nanocomposites: electrical properties under dc and ac fields. *Synthetic metals, 160*(15-16), 1718-1726.

Zidan, H.M., Abu-Elnader, M. (2005). Structural and optical properties of pure PMMA and metal chloride-doped PMMA films. *Physica B: Condensed Matter, 355*(1-4), 308-317.